



Contents list available at IJRED website

International Journal of Renewable Energy Development

Journal homepage: <https://ijred.undip.ac.id>



Research Article

Enhancing Ionic Conductivity of Carboxymethyl Cellulose-Lithium Perchlorate with Crosslinked Citric Acid as Solid Polymer Electrolytes for Lithium Polymer Batteries

Akhiruddin Maddu^{a*}, Ahmad Sofyan Sulaeman^b, Setyanto Tri Wahyudi^a,
Abdulloh Rifai^c

^aDepartment of Physics, IPB University, Indonesia

^bDepartment of Physics, Faculty of Science, Universitas Mandiri, Indonesia

^cResearch Center for Advanced Materials, National Research and Innovation Agency (BRIN), Indonesia

Abstract. Lithium batteries development are triggered so many efforts in producing electronic devices due to its excellent performance as energy storage systems. One of the appealing points solid polymer electrolytes for developing solid-state lithium batteries. In this study, Solid polymer electrolytes with crosslinked treatment (SPE-C) were prepared from carboxymethyl cellulose-lithium perchlorate (CMC-LiClO₄) and citric acid (CA) as a crosslinker via solution casting method. All SPE-C membranes were assembled into lithium battery coin cells. Degree of crosslinked and degradation were measured to observe crosslink formation in SPE-C membranes and confirmed by fourier transform infrared (FTIR), whereas SPE-C in coin cells were characterized by electrochemical impedance spectroscopy (EIS) and linear sweep voltammograms (LSV). The results showed that crosslinked process is successfully obtained with C=O from ester linkage of CA vibration within COO⁻ of CMC for the crosslinking bond formation. The crosslink effect also contributed on enhancing ionic conductivities of SPE-C in coin cells from EIS results. The highest ionic conductivity was obtained in SPE-C2 (1.24×10⁻⁷ S/cm) and electrochemically stable in 2.15 V based on LSV measurement. SPE-C2 has good dielectric behavior than the others due to the high ions mobilities for migration process from ion clusters formation, thus it would be useful for further study in obtaining the powerful solid-state lithium polymer batteries.

Keywords: solid polymer electrolytes, carboxymethyl cellulose, crosslink, ionic conductivity, lithium polymer batteries.



@ The author(s). Published by CBIORE. This is an open access article under the CC BY-SA license (<http://creativecommons.org/licenses/by-sa/4.0/>)

Received: 15th July 2021; Revised: 17th Nov 2021; Accepted: 20th June 2022; Available online: 12th July 2022

1. Introduction

The efforts on rechargeable lithium batteries development as energy storage systems for several electronic devices still have much attention. Various ideas were developed to improve battery performance, such as high energy density, high capacity, and long lifespan with a specific study on each battery component (Fu *et al.* 2016). One of the components that has been extensively researched for solid-state battery development is solid polymer electrolytes (SPE) (Ali & Mohammed, 2020).

SPE have been paid much attention for solid-state lithium batteries application due to ensuring its safety such as non-volatile, low flammability, and electrochemically stable (Ben youcef *et al.* 2016). Another advantage in SPE is design flexibility due to easier processability (Arya *et al.* 2019; Scrosati & Garche, 2010; Tarascon & Armand, 2001). Several polymers which can be used as hosts for SPE preparation are divided into two types, namely synthetic and natural polymers (Aziz *et al.*

2019; Nyuk & Isa, 2017). polymethylmethacrylate (Chen & Vereecken, 2019), polycarbonate (Sun *et al.* 2014), polyacrylonitrile (Verdier *et al.* 2020), polyethylene oxide (Yap *et al.* 2013), and poly vinyl alcohol (Saadiah & Samsudin, 2018) are synthetic polymers, whereas starch (Ma *et al.* 2007), carrageenan (Ghani *et al.* 2019), pectin (Perumal *et al.* 2019), chitin (Shyly *et al.* 2014), lignocellulosic (Ren *et al.* 2020), sago (Samsudin *et al.* 2012), chitosan (Aziz *et al.* 2019), and cellulose (Samsudin *et al.* 2014) are known as natural polymers that can be used for SPE preparation.

However, several disadvantage issues, such as non-biodegradable, expensive price, and disposal issues about synthetic polymers made a new perspective from researchers to use natural polymers as SPE (Baharun *et al.* 2018; Salleh *et al.* 2016). Cellulose-based SPE such as carboxymethyl cellulose (CMC) is a famous polymer with marvelous characteristics for battery application based on previous studies (Nyuk & Isa, 2017; Samsudin *et al.* 2014; Sulaeman *et al.* 2021). CMC is a biodegradable material,

* Corresponding author:
Email: akhiruddin@apps.ipb.ac.id (A. Maddu)

low cost, non-toxic to the environment, and exhibits good film-forming ability (Mazuki *et al.* 2020; Megha *et al.* 2018; Putro *et al.* 2019). It has been studied in a lots of works which developed CMC in the electrolytes system with promising conduction properties (Mazuki *et al.* 2020; Mazuki *et al.* 2019). However, another obstacle, like the appearance of dendrite is one of the factors that disturb safety in the battery system (Ben youcef *et al.* 2016; Wang *et al.* 2018), because the need for batteries with high energy density certainly requires a stable SPE system.

An effort that can be conducted to ensure the stability of SPE is adding a crosslinker (Chaudoy *et al.* 2016; Lehmann *et al.* 2020; Meabe *et al.* 2019), because crosslinker has proven to increase the stability and storage modulus of SPE (Ben youcef *et al.* 2016). In addition, the presence of crosslinker could increase the dissociation most of unpaired anions exist in the crosslinked network (Elmore *et al.* 2018). CA is one of the candidates that can crosslinked CMC structure. It forms a cyclic anhydride and esterifies the hydroxyl groups in the polymer chains (Mali *et al.* 2018), thus the crosslinked process were obtained and increase the ionic dissociation to enhance the ionic conductivity.

In the present scenario, we provide a new class crosslinked SPE (SPE-C) from CMC and LiClO₄ used as host polymer and ionic salt, respectively. The CMC-LiClO₄ mixtures are crosslinked by CA addition. The utilization of CMC and LiClO₄ and the addition of Citric acid as crosslinker for SPE has never been reported before. SPE-C is successfully synthesized based on the degree of crosslinking measurement which is confirmed by FTIR results. Moreover, we observed the dielectric behavior from several parameters (e.g. complex impedance, dielectric permittivity, ionic conductivity, loss tangent, and electrical modulus) that had never been done in this SPE-C before based EIS method. Furthermore, the voltage stability of SPE-C in battery cell also analyzed via LSV measurement.

2. Materials and Methods

2.1 Materials and SPE-C membranes preparation

Carboxymethyl Cellulose (D.S: 0.98, Viscosity: ≥1900 Pa.s) and Citric Acid technical grade (Mw: 192.12 g/mol) were obtained from Alibaba.com. Lithium Perchlorate (LiClO₄ Purity: 97.0% analytical grade) were purchased from KANTO CHEMICAL CO., INC, Japan. The SPE-C membranes preparation were briefly displayed in Fig. 1. In the preparation process, CMC was added into 30 mL to a solid content of 2 wt% and stirred at 50 °C for 6 hours. Then, 20 wt% LiClO₄ was added to CMC solution under stirring process until homogenous solution was obtained. To obtain the SPE-C membranes, CA was dissolved into CMC-LiClO₄ solution to the desired weight ratio (0 wt%, 5 wt%, and 10 wt%) and named as shown at Table 1. The mixed solution was casted on a petri dish (60 mm x 15 mm) and dried at 40 °C overnight for water evaporation and continued to 24 hours for drying process in desiccator (Capanema *et al.* 2018). The prepared membranes were cut into a square (10 × 10 mm) and circular pieces (d = 19 mm) and stored in a vacuum desiccator for stabilizing their mass. The square SPE-C samples were characterized by their degree of crosslinking and degradation in water and FTIR measurement, whereas circular SPE-C were prepared for assembly process with lithium metal electrodes and punched to obtain coin cells. The cells were

stored in vacuum desiccator for next characterization as EIS and LSV.

2.2 Characterization

2.2.1 Degree of Crosslinked and Degradation

SPE-C membranes were immersed in water for 1 hour and heated at 50 °C for 10 minutes to get the dried films. We measured the initial weight (W_i) and dry weight after immersing (W_a) during the process. After that, we calculated all quantities to obtain Degree of Crosslinking (DC) (Wivanius & Budianto, 2015) and Degree of Degradation (DD) (Capanema *et al.* 2018) by using equation (1) and (2).

$$DC (\%) = \frac{W_a}{W_i} \times 100\% \quad (1)$$

$$DD (\%) = \frac{W_i - W_a}{W_a} \times 100\% \quad (2)$$

2.2.2 Molecular vibration

Fourier transform infrared (FTIR) spectra of SPE-C membranes were taken by Nicolet iS-10 Smart iTR 500-4000 FT-IR spectrophotometer with ATR accessory for molecular vibration identification in the range 4000 – 400 cm⁻¹ wavenumber with scanning resolution of 0.5 cm⁻¹.

2.2.3 Electrochemical properties

Electrochemical impedance spectroscopy (EIS) (Methrohm Autolab with Nova 1.11 software) was used to observe some electrical parameters as complex impedance plots. The circular SPE-C through an assembly process in glove box (Vigor Tech, USA) with lithium metal electrodes (Li⁺/SPE-C/Li⁺) and crimped to obtain coin cells (CR 2032 3V lithium cell). The cells were stored in vacuum desiccator. EIS also can interprets in various parameters such as dielectric permittivity, ionic conductivity, phase angel, and electrical modulus of SPE-C following equations (3), (4), (5), (6), (7), and (8), respectively (Aziz *et al.* 2018; Aziz *et al.* 2019).

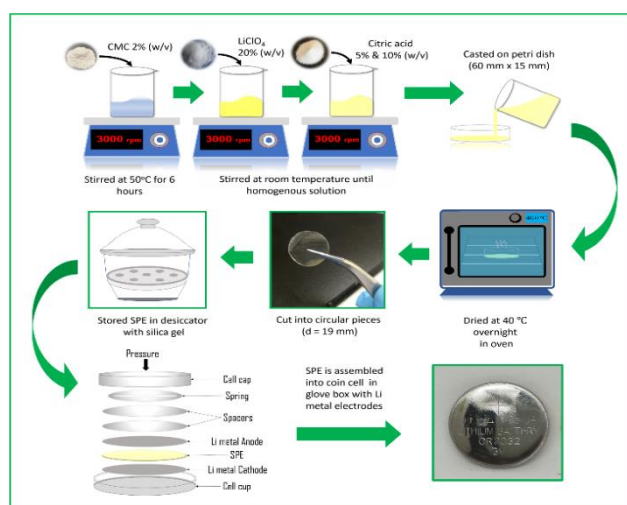


Fig. 1 Schematic representation of SPE-C synthesis following with lithium battery coin cells preparation.

Table 1

Various composition of the samples.

| Sample names | Description |
|--------------|---|
| SPE-C0 | 2 wt% CMC + 20 wt% LiClO ₄ |
| SPE-C1 | 2 wt% CMC + 20 wt% LiClO ₄ + 5 wt% CA |
| SPE-C2 | 2 wt% CMC + 20 wt% LiClO ₄ + 10 wt% CA |

$$\epsilon' = \frac{z''}{\omega C_0(z'^2 + z''^2)} \quad (3)$$

$$\epsilon'' = \frac{z'}{\omega C_0(z'^2 + z''^2)} \quad (4)$$

$$\sigma_{DC} = \frac{t}{R_b \times A} \quad (5)$$

$$\tan \delta = \frac{\epsilon''}{\epsilon'} \quad (6)$$

$$M' = \frac{\epsilon'}{(\epsilon')^2 + (\epsilon'')^2} \quad (7)$$

$$M'' = \frac{\epsilon''}{(\epsilon')^2 + (\epsilon'')^2} \quad (8)$$

Where, ϵ' , ϵ'' , σ_{DC} , t , R_b , A , $\tan \delta$, M' , and M'' are real dielectric, imaginary dielectric, real impedance, imaginary impedance, ionic conductivity, thickness, bulk resistance, surface area, loss tangent, real electrical modulus, and imaginary electrical modulus, respectively. Meanwhile, ω and C_0 are angular frequency and capacitance in vacuum. ω is given by $2\pi f$ where f is frequency of applied field, whereas C_0 is given by $\epsilon_0 A/L$. ϵ_0 , A , and L is permittivity of free space (8.854×10^{-14} F cm⁻¹), surface area and thickness of the samples, respectively (Aziz 2013; Aziz *et al.* 2018; Aziz & Mamand, 2018; Aziz *et al.* 2020).

2.2.4 Potential stability

The SPE-C in coin cells are further studied by using linear sweep voltammogram (LSV) to identify their voltage stability and decomposition. The coin cells were placed at circular electrode and measured by using (WBCS 3000 battery cycler) with 5 mV.s⁻¹ scan rates under AC voltage.

3. Results and Discussion

3.1 Molecular vibration

The molecular vibration of each sample from FTIR spectra were given by Fig. 1. In the functional group region, the broad-strong, low, and sharp peaks at 3363 cm⁻¹, 2928 cm⁻¹, and 1588 cm⁻¹ in all SPE-C samples are assigned as O-H vibration, C-H bands, and asymmetric COO⁻ group, respectively (Capanema *et al.* 2018; Ghorpade *et al.* 2018; Gupta & Varshney, 2019; Kanafi *et al.* 2019; Ndruru *et al.* 2019). In addition, in the finger print region, the stretching, symmetrical stretching at 1417 cm⁻¹ and 1325 cm⁻¹ assigned as O-H and C-H groups (Gupta & Varshney, 2019). The vibration at 1269 cm⁻¹ is carboxyl groups (-COOH), which are assigned to antisymmetric stretching vibration between (C=O) and (C-O) from CMC and CA (Capanema *et al.* 2018).

However, the contrast of FTIR spectra between SPE-C0, SPE-C1, and SPE-C2 is can be seen at Fig. 2b. Another vibration peak which are identified at 1730 cm⁻¹ represents

ester C=O stretching from CA. (Mali *et al.* 2018) claimed that the presence of C=O and COO⁻ is confirmed as crosslinking formation between CMC and CA in SPE-C1 and SPE-C2 system. Meanwhile, the contribution of LiClO₄ in all SPE-C is assigned at 1054 cm⁻¹ with spectroscopically free ClO₄⁻ ions. The stretching at 898 cm⁻¹ is the presence of 81-4 glycoside bonds between glucose units (Abarna & Hirankumar, 2014; Capanema *et al.* 2018; Sim *et al.* 2010; Sunandar *et al.* 2019).

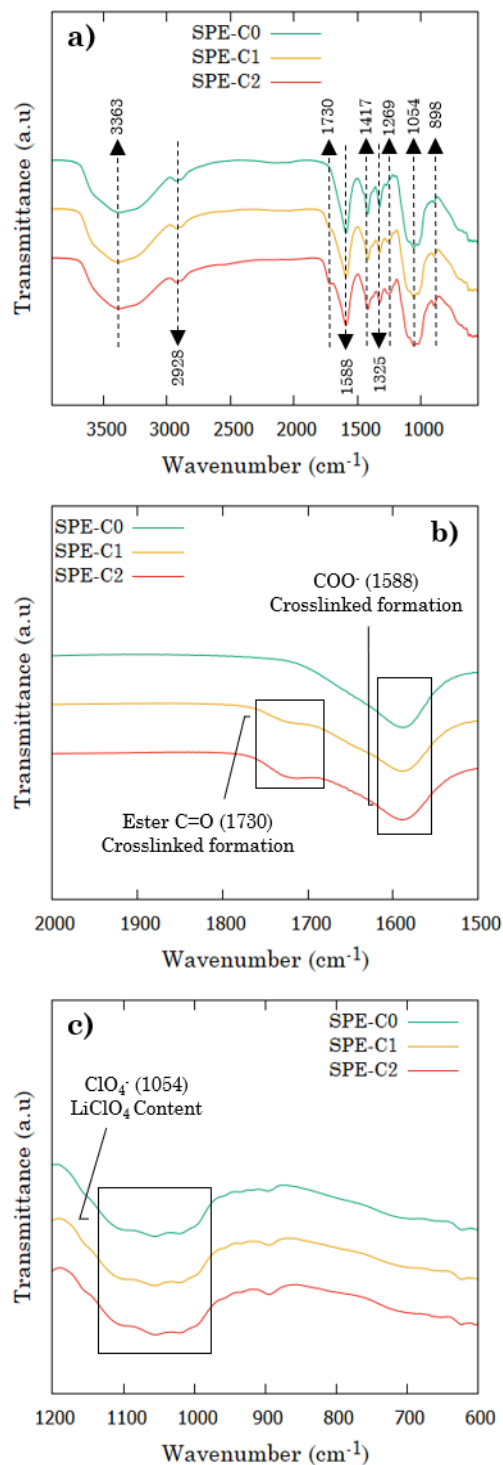


Fig. 2 FTIR spectra of a) SPE-C0, SPE-C1, and SPE-C2; b) C=O and COO⁻ stretching region (2000 cm⁻¹ – 1500 cm⁻¹); c) ClO₄⁻ stretching region (1200 cm⁻¹ – 600 cm⁻¹).

3.2 Degree of crosslinking and Degree of degradation

Degree of crosslinking (DC) and Degree of degradation (DD) percentage were measured to prove the crosslinked formation in SPE-C structure. The crosslinked formation is signified by a formation of covalent bond bridging the functional groups of the polymer chain, thus the SPE-C with CA addition as a crosslinker have a more rigid structure and not easily degraded when it is immersed in water (Capanema et al. 2018; Mali et al. 2018). As we can see in Fig. 3, various DC and DD percentage were obtained from all samples. The DC percentage of SPE-C0 without CA addition as crosslinker is 12.5 %. Then, it is increased significantly to 63.8 % in SPE-C1 with 5 wt% CA addition. In the SPE-C2 sample, the DC percentage increased slightly to 72.22 % at the addition of 10 wt% CA.

The crosslinked formation in SPE-C is influenced by –COOH groups of CMC (Nan et al. 2019). CMC with high D.S value (i.e., D.S: 1.22) has a higher –COOH groups that affected the crosslinked process with CA addition. In previous study, (Capanema et al. 2018) needs 25 wt% CA addition to crosslink CMC with 1.22 D.S value, because –COOH as hydrophilic molecules with negative charges species may have caused the repulsion between contiguous polymer chains and obstruct the crosslinking process with hydroxyl groups. However, the D.S of CMC which was used in this study is 0.98, thus SPE-C0 still has DC value without CA addition, then 5 wt% and 10 wt% CA addition are enough for crosslinking formation of SPE-C1 and SPE-C2, significantly.

Furthermore, DD measurement is obtained to ensure that all of SPE-C samples is not fully crosslinked. The DD percentage of SPE-C0 achieve to 87.5 % without CA addition. Meanwhile, the DD percentage decreased to 36.20 %, and 27.77 % for SPE-C1 and SPE-C2, respectively. It means that the high DD percentage in SPE-C0 confirmed an ease of the sample to degrade due to high interaction between –COOH and water without the presence crosslinker component from CA as it describes before. Thus, SPE-C0 has a weak structure that can influence its performance in lithium batteries system. Besides, the increment of DD percentage in SPE-C1 and SPE-C2 is caused by the limitation from their structure in loading water. It means that both of these samples have high endurance than SPE-C0.

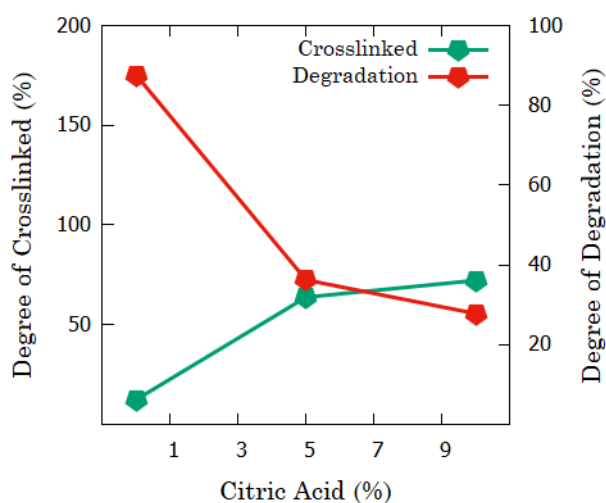


Fig. 3 Degree of crosslinked and Degree of degradation for SPE-C with different CA concentration.

3.3 Complex impedance plots

The study of complex impedance plots is a powerful tool to investigate the phase lag of charge carrier’s movement under ac voltage. It is an outstanding informative on demonstrating the resistances of SPE-C and obtaining its ionic conductivity (Aziz et al. 2018; Stavrinidou et al. 2014). Nyquist plot displayed with imaginary (Z'') and the real (Z') parts of the complex impedance as shown in Fig. 4.

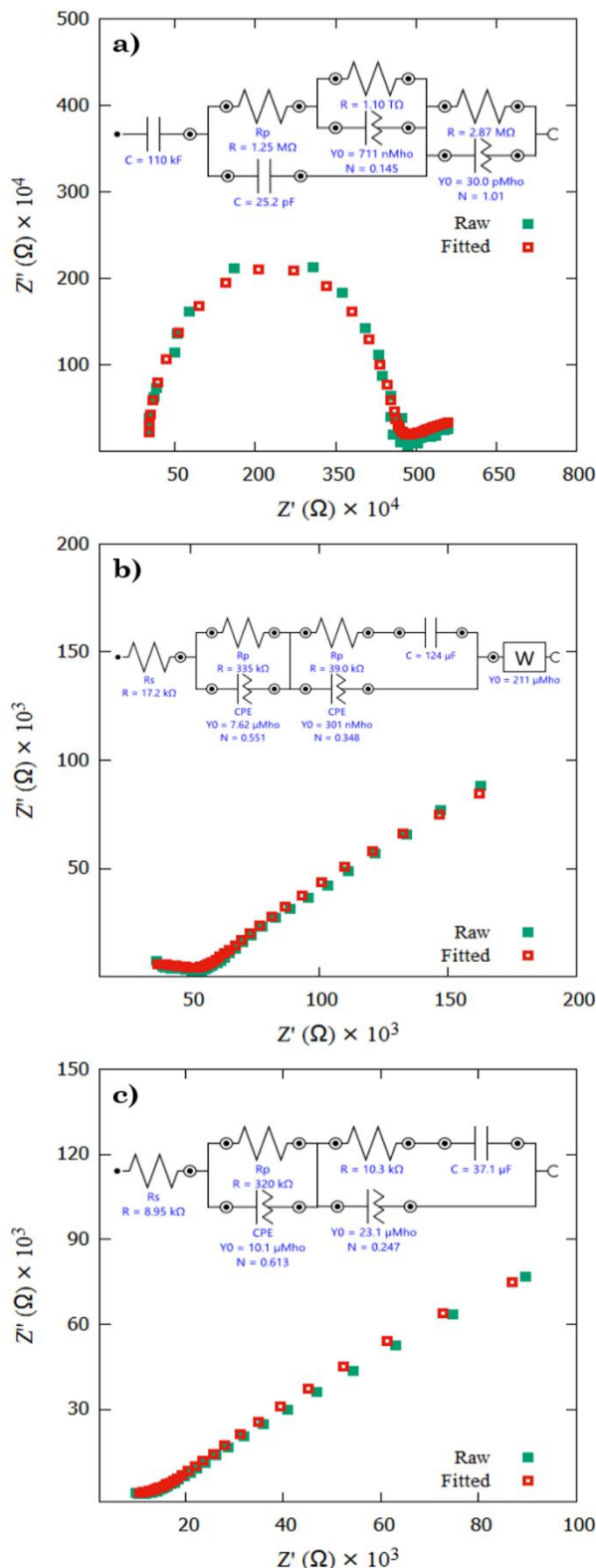


Fig. 4 Complex impedance plots of a)SPE-C0, b)SPE-C1, and c)SPE-C2 fitted with electrical equivalent circuits (EECs) models.

A distinctive result is performed by Fig. 4a due to the high semi-circle is resulted by SPE-C0. The high impedance result in SPE-C0 indicates high charge-transfer resistance due to the low Li ion conduction process through the bulk of SPE-C0 (Aziz *et al.* 2018; Mei *et al.* 2018). This situation is confirmed by EECs model that produce three parallel circuits with high values of impedance components as shown in Fig. 4a, thus it neither of charge-transfer in electrode surface and resulted a slightly Li ions diffusion through SPE-C0 (Yuan *et al.* 2010). However, the semi-circle is depressed in SPE-C1 and SPE-C2 following an increment of impedance components values with Warburg impedance formation. Warburg impedance is known as ions injection and diffusion inside the SPE-C system (Stavriniidou *et al.* 2014). These results may be assumed that CA addition in SPE-C1 and SPE-C2 build up the complete polymer species such as C=O and COO⁻ formation to dissociate LiClO₄ by using oxygen species. Therefore, Li ions can diffuse through SPE-C1 and SPE-C2 system better than in SPE-C0.

3.4 Complex dielectric permittivity

Dielectric permittivity is helpful to observe the polarizing ability and ion dynamics in SPE-C due to the roles of salts and polymer chains under external electric fields (Arya *et al.* 2019; Arya & Sharma, 2018b). The role of ϵ' (Fig. 5a) is assigned as the capacitance of SPE-C and measures the polarization, whereas ϵ'' (Fig. 5b) is assigned as the energy required for the polarization process (Aziz *et al.* 2018). The ϵ' and ϵ'' curves have a similar pattern for all samples which is the permittivity values are high at low frequency and decrease gradually at higher frequency. From these two graphs (Fig. 5a & Fig. 5b), the high permittivity at low frequency region is caused by charge accumulation process in electrode-electrolyte interface or called as electrode polarization (Putro *et al.* 2021; Sulaeman *et al.* 2021). Furthermore, the permittivity has decrease at intermediate frequency due to the alteration of molecular dipoles depended to field. The constant ϵ' and ϵ'' long tail curves are at higher frequency indicated the lack of excess ion diffusion due to fast polarity of field in high frequency or called as dielectric relaxation process (Aziz *et al.* 2019; Ravi *et al.* 2016).

SPE-C0 showed low ϵ' and ϵ'' due to high resistance. It indicates the presence of ionic pairing effect when polarization process among electrode-electrolyte interface, thus a low ϵ' and ϵ'' is linearly related with low ionic conductivity as presented at Table 1. However, the ϵ' and ϵ'' enhanced at SPE-C1 and SPE-C2 because both decrease their resistance due to the 5 wt% and 10 wt% CA addition, respectively. The enhancement of ϵ' and ϵ'' is influenced by high charge density when polarization process between electrode-electrolyte interface (Arya & Sharma, 2018b; Ravi *et al.* 2016), thus it resulted a dense activity of charge and charge carriers in accumulation process to align the dipoles and released the ions to result high ionic conductivities.

Table 2

Electrical parameter values of SPE-C from EIS characterization.

| Samples names | Electrical parameters (R_b , σ_{DC} , and ϵ') | | |
|---------------|---|-----------------------|-------------|
| | R_b (Ω) | σ_{DC} (S/cm) | ϵ' |
| SPE-C0 | 3.83×10^6 | 2.44×10^{-9} | 96.68 |
| SPE-C1 | 3.43×10^5 | 3.71×10^{-8} | 536.81 |
| SPE-C2 | 6.18×10^4 | 1.24×10^{-7} | 1964.42 |

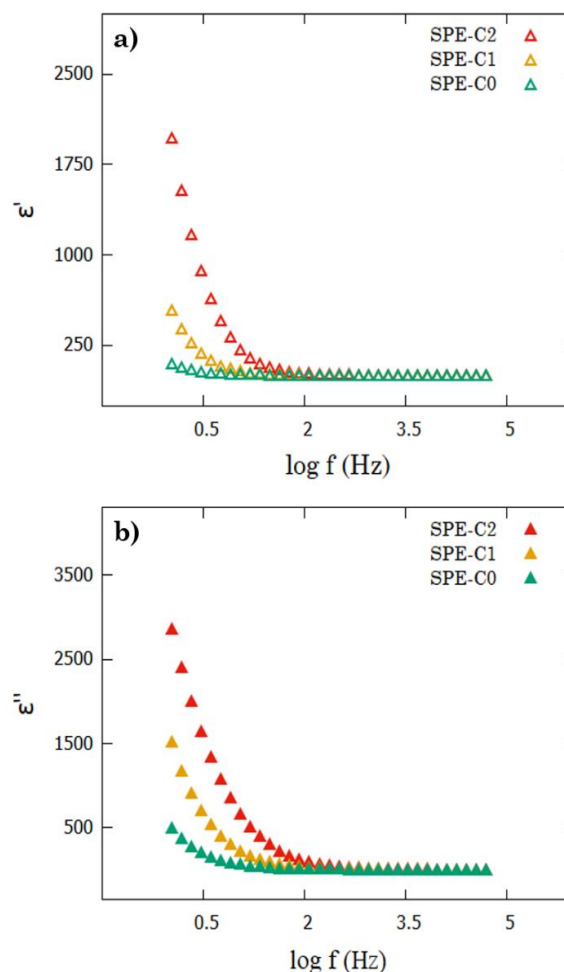


Fig. 5 The real a) and imaginary b) parts of dielectric permittivity as a function of frequency.

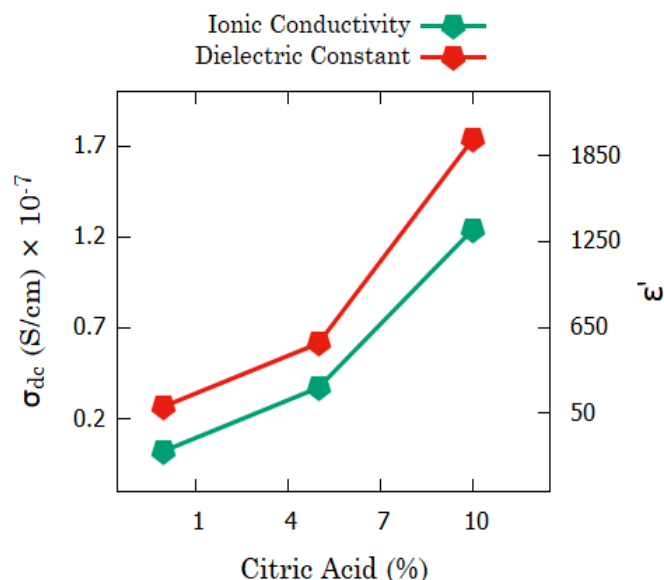


Fig. 6 Various σ_{DC} and ϵ' values depend to CA concentration.

3.5 Ionic conductivity and dielectric constant

The ionic conductivity against dielectric constant of all SPE-C samples which depended to CA concentration is presented in Fig. 6. The various ionic conductivities of SPE-C with or without CA addition are shown in Table 2,

following the specific value of σ_{DC} , R_b , and ε' . SPE-C0 shows lowest σ_{DC} than other samples. It is caused by the lack of dielectric activities in SPE-C0 that triggered ionic pairs effect from the coulombic interaction between polymer matrix and LiClO_4 salts (Aziz & Abidin, 2013; Ng *et al.* 2011). Therefore, this phenomenon resulted a high R_b value and limited the Li ion diffusion in SPE-C0. Meanwhile, the increase of σ_{DC} with increasing CA concentration indicated that CA in SPE-C1 and SPE-C2 can composed the Li ions between LiClO_4 salt and polymer matrix to diffuse through the SPE-C1 and SPE-C2 system. This situation is confirmed in FTIR results (Fig. 2) that CA influenced LiClO_4 dissociation based on the enhancement of ClO_4^- free ions. The composed of free ions in SPE-C1 and SPE-C2 leads to ion clusters formation with their charge carriers, thus they enhance ions mobility for migration process (Badry *et al.* 2021; Chai & Isa, 2011). Therefore, the σ_{DC} in SPE-C1 and SPE-C2 increased with increasing CA concentration.

3.6 Loss tangent analysis

The plotted $\tan \delta$ (Fig. 7) aims to understand the relaxation process (Aziz *et al.* 2020). The shapes of $\tan \delta$ plots increase with increasing frequency until a maximum peak and decrease at higher frequency based on Koop's phenomenological model (Koops 1951). It caused that ohmic component at low frequency is higher than its capacitive component, whereas the capacitive component is high at higher frequency (Aziz *et al.* 2020; Koops 1951). The presence of single peak in all SPE-C shows the ion migration via polymer segmental motion (Arya *et al.* 2019). A high peak at SPE-C0 in the middle frequency is assumed as high dielectric relaxation due to the long-range migration. Meanwhile, a dual-phase ions migration experienced at SPE-C1 at intermediate and high frequency is a migration of ions via short-range with increasing ionic conductivity (Tripathi *et al.* 2020). Furthermore, we obtain a shifting peak at SPE-C2 which is claimed to reduce dielectric relaxation due to the case related to previous results carried out by (Putro *et al.* 2021). They explained that the shifts of $\tan \delta$ ensure a high conductivity due to the high charge density in SPE-C2. It is similar to our complex dielectric and impedance results.

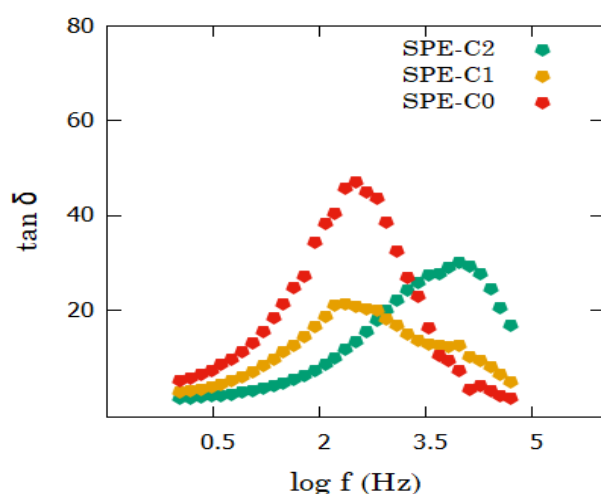


Fig. 7 Various $\tan \delta$ curves of SPE-C0, SPE-C1 and SPE-C2 as a function of frequency.

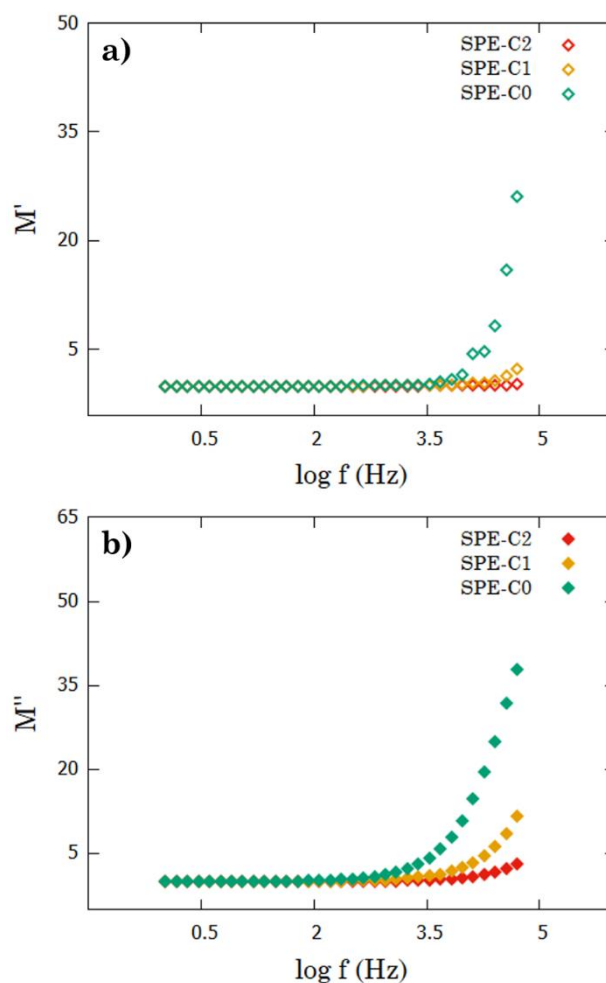


Fig. 8 The real (a) and imaginary (b) parts of electrical modulus as a function of frequency.

3.7 Electrical modulus

In this section, the conductivity mechanism is specifically described on electrical modulus (Fig. 8). This analysis depicts bulk dielectric behavior in all SPE-C samples such as conductivity relaxation process and ion hopping mechanism (Verma & Sahu, 2017). Similar curves of all samples are provided in this study where M' (Fig. 8a) and M'' (Fig. 8b) values approach to zero at low frequency and increase at higher frequency. M' values at low frequency assigned as electrode polarization process due to large double layer capacitance association (Arya & Sharma, 2018a), then the ions are dispersed in high frequency and resulted in an increase of M' . Therefore, the ions achieved a relaxation process in segmental polymer chain (Tripathi *et al.* 2020).

SPE-C0 has a higher M' values that informed a long conduction relaxation than SPE-C1 and SPE-C2 where both have a short conduction relaxation with low M' in high frequency. This dispersion in the M' of the modulus corresponds to the peak in the M'' of the modulus spectra. M'' increases with increasing frequency is related to the long-range random hopping of ions in the material, which reaches to a maximum value at a particular frequency. It relates to conduction relaxation process in SPE-C, where long-range motion is restricted to caged motion. The long-range motion belongs to the sample with a higher M'' whereas the samples with low M'' have a short-range ion

motion and resulting in short relaxation process (Kumar & Srivastava, 2015; Verma & Sahu, 2017). In our results, CA concentration influenced the relaxation process that contributes to polymer chain complexation via C=O and COO⁻ groups for facilitating the ionic transport in SPE-C1 and SPE-C2. Therefore, these results were linear with ionic conductivity and dielectric constant values in previous section that high electrical modulus in high frequency describes as long dielectric relaxation which is caused by low ionic conductivity and dielectric constant, whereas low electrical modulus is triggered by high ionic conductivity and its dielectric constant.

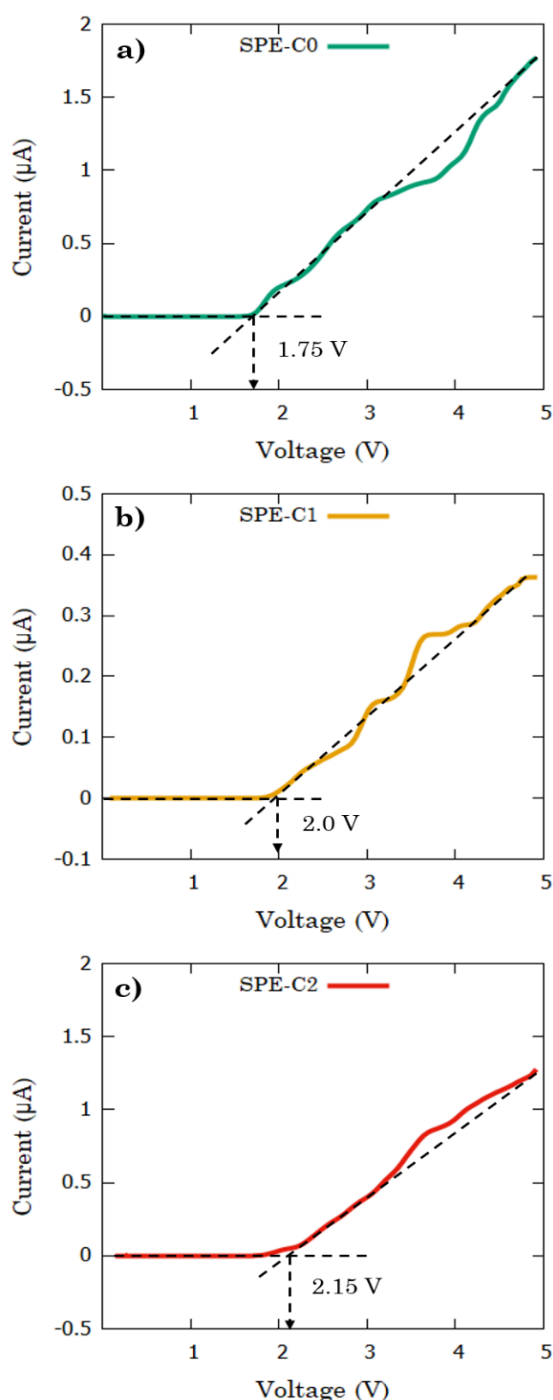


Fig. 9 LSV curves with decomposition voltage points of SPE-C0 a), SPE-C1 b), and SPE-C2 c).

3.8 Linear sweep voltammogram

LSV analysis played a crucial role in determining the potential stability and decomposition of SPE-C in battery cells (Dannoun *et al.* 2020). The LSV measurement was carried out using 5 mV.s⁻¹ scan rate, as shown in Fig. 9. The LSV curves performed in current versus voltage which are initiated with a straight line and finished with voltage breakdown (drastic increase line). In this case, a straight line represents electrochemical stability, while a drastic increase line is claimed as decomposition voltage of SPE-C (Abidin *et al.* 2012).

Three samples have a different decomposition voltage from each other. SPE-C2 (Fig. 9c) has more voltage stability (2.15 V), whereas SPE-C0 (Fig. 9a) and SPE-C1 (Fig. 9b) have 1.75 V and 2.0 V voltage stabilities, respectively. We observed that CA addition successfully enhanced the electrochemical stability, similar with the previous result studied by (Jiang *et al.* 2019). They claimed that polymer chain structure of SPE-C's stable polymer chain structure is caused by crosslinker addition, therefore the voltage stability and decomposition of SPE-C increase.

4. Conclusion

The crosslinked SPE-C-based CMC-LiClO₄ is successfully prepared with CA addition as crosslinker. The degree of crosslinking measurement showed that SPE-C2 has a higher crosslinked degree (72.22%) with 10% CA addition. The functional groups of each other materials contribute to building up the crosslink formation and LiClO₄ dissociation to form free ions. Based on calculation from EIS data, SPE-C2 has a higher ionic conductivity at 1.24×10^{-7} S/cm and good dielectric behavior than the others due to the high ions mobilities for migration process from ion clusters formation. Meanwhile, the voltage stability of SPE-C2 is over 2 V in LSV results, it is caused by crosslinker addition on polymer chain structure.

Acknowledgments

The authors appreciatively acknowledge the facilities as laboratory for experimental and characterization from Battery Research Group of Research Centre for Physics, Indonesian Institute of Sciences.

Dedication

Dedicated to Doctor Bambang Prihandoko who passed away on June 11st, 2021 at the age of 55th years.

References

- Abarna, S., & Hirankumar, G. (2014). Study on new lithium ion conducting electrolyte based on polyethylene glycol – p-tert-octyl phenyl ether and lithium perchlorate. *International Journal of ChemTech Research*, 6(13), 5161–5167.
- Abidin, S. Z. Z., Hassan, O. H., Ali, A. M. M., & Yahya, M. Z. A. (2012). Electrochemical studies on cellulose acetate-LiBOB polymer gel electrolytes. *International Journal of Electrochemical Science*, 8, 7320–7326. <http://www.electrochemsci.org/papers/vol8/80507320.pdf>
- Ali, B., & Mohammed, A. B. R. (2020). Ionic conductivity of chitosan-lithium electrolyte in biodegradable battery cell. *Indonesian Journal of Chemistry*, 20(3), 655–660;

- doi:10.22146/ijc.45283
- Arya, A., Sadiq, M., & Sharma, A. L. (2019). Salt concentration and temperature dependent dielectric properties of blend solid polymer electrolyte complexed with NaPF₆. *Materials Today: Proceedings*, 12(3), 554–564; doi:10.1016/j.matpr.2019.03.098
- Arya, A., & Sharma, A. L. (2018a). Effect of salt concentration on dielectric properties of Li-ion conducting blend polymer electrolytes. *Journal of Materials Science: Materials in Electronics*, 29(20), 17903–17920; doi:10.1007/s10854-018-9905-3
- Arya, A., & Sharma, A. L. (2018b). Structural, electrical properties and dielectric relaxations in Na⁺-ion-conducting solid polymer electrolyte. *Journal of Physics Condensed Matter*, 30(16), 165402; doi:10.1088/1361-648X/aab466
- Aziz, S. B. (2013). Li⁺ ion conduction mechanism in poly (ϵ -caprolactone)-based polymer electrolyte. *Iranian Polymer Journal*, 22(12), 877–883; doi:10.1007/s13726-013-0186-7
- Aziz, S. B., Abdullah, O. G., Saeed, S. R., & Ahmed, H. M. (2018). Electrical and dielectric properties of copper ion conducting solid polymer electrolytes based on chitosan: CBH model for ion transport mechanism. *International Journal of Electrochemical Science*, 13(4), 3812–3826; doi:10.20964/2018.04.10
- Aziz, S. B., & Abidin, Z. H. Z. (2013). Electrical conduction mechanism in solid polymer electrolytes: New concepts to arrhenius equation. *Journal of Soft Matter*, 2013, 323868; doi:10.1155/2013/323868
- Aziz, S. B., Faraj, M. G., & Abdullah, O. G. (2018). Impedance spectroscopy as a novel approach to probe the phase transition and microstructures existing in CS:PEO based blend electrolytes. *Scientific Reports*, 8(14308), 1–14; doi:10.1038/s41598-018-32662-1
- Aziz, S. B., Hamsan, M. H., Abdullah, R. M., & Kadir, M. F. Z. (2019). A promising polymer blend electrolytes based on chitosan: Methyl cellulose for EDLC application with high specific capacitance and energy density. *Molecules*, 24(13), 2503; doi:10.3390/molecules24132503
- Aziz, S. B., Karim, W. O., & Ghareeb, H. O. (2020). The deficiency of chitosan: AgNO₃ polymer electrolyte incorporated with titanium dioxide filler for device fabrication and membrane separation technology. *Journal of Materials Research and Technology*, 9(3), 4692–4705; doi:10.1016/j.jmrt.2020.02.097
- Aziz, S. B., & Mamand, S. M. (2018). The Study of dielectric properties and conductivity relaxation of ion conducting chitosan: NaTf based solid electrolyte. *International Journal of Electrochemical Science*, 13(11), 10274–10288; doi:10.20964/2018.11.05
- Aziz, S. B., Marif, R. B., Brza, M. A., Hamsan, M. H., & Kadir, M. F. Z. (2019). Employing of Trukhan model to estimate ion transport parameters in PVA based solid polymer electrolyte. *Polymers*, 11(10), 1694; doi:10.3390/polym11101694
- Badry, R., Ezzat, H. A., El-Khodary, S., Morsy, M., Elhaes, H., Nada, N., & Ibrahim, M. (2021). Spectroscopic and thermal analyses for the effect of acetic acid on the plasticized sodium carboxymethyl cellulose. *Journal of Molecular Structure*, 1224, 129013; doi:10.1016/j.molstruc.2020.129013
- Baharun, N. N. S., Mingsukang, M. A., Buraidah, M. H., Woo, H. J., & Arof, A. K. (2018). Electrical properties of plasticized sodium-carboxymethylcellulose (NaCMC) based polysulfide solid polymer electrolyte. *International Conference on Transparent Optical Networks (ICTON), 2018-July*, 1–4; doi:10.1109/ICTON.2018.8473830
- Ben youcef, H., Garcia-Calvo, O., Lago, N., Devaraj, S., & Armand, M. (2016). Cross-linked solid polymer electrolyte for all-solid-state rechargeable lithium batteries. *Electrochimica Acta*, 220, 587–594; doi:10.1016/j.electacta.2016.10.122
- Capanema, N. S. V., Mansur, A. A. P., de Jesus, A. C., Carvalho, S. M., de Oliveira, L. C., & Mansur, H. S. (2018). Superabsorbent crosslinked carboxymethyl cellulose-PEG hydrogels for potential wound dressing applications. *International Journal of Biological Macromolecules*, 106, 1218–1234; doi:10.1016/j.ijbiomac.2017.08.124
- Chai, M. N., & Isa, M. I. N. (2011). Carboxyl methylcellulose solid polymer electrolytes : Ionic conductivity and dielectric study. *Journal of Current Engineering Research*, 1(2), 1–5.
- Chaudoy, V., Ghamouss, F., Luais, E., & Tran-Van, F. (2016). Cross-linked polymer electrolytes for li-based batteries: From solid to gel electrolytes. *Industrial and Engineering Chemistry Research*, 55(37), 9925–9933; doi:10.1021/acs.iecr.6b02287
- Chen, X., & Vereecken, P. M. (2019). Solid and solid-like composite electrolyte for lithium ion batteries: Engineering the ion conductivity at interfaces. *Advanced Materials Interfaces*, 6(1), 1800899; doi:10.1002/admi.201800899
- Dannoun, E. M. A., Aziz, S. B., Brza, M. A., Nofal, M. M., Asnawi, A. S. F. M., Yusof, Y. M., Al-Zangana, S., Hamsan, M. H., Kadir, M. F. Z., & Woo, H. J. (2020). The study of plasticized solid polymer blend electrolytes based on natural polymers and their application for energy storage EDLC devices. *Polymers*, 12(11), 2531; doi:10.3390/polym12112531
- Elmore, C. T., Seidler, M. E., Ford, H. O., Merrill, L. C., Upadhyay, S. P., Schneider, W. F., & Schaefer, J. L. (2018). Ion transport in solvent-free, crosslinked, single-ion conducting polymer electrolytes for post-lithium ion batteries. *Batteries*, 4(2), 1–17; doi:10.3390/batteries4020028
- Fu, K., Gong, Y., Dai, J., Gong, A., Han, X., Yao, Y., Wang, C., Wang, Y., Chen, Y., Yan, C., Li, Y., Wachsmann, E. D., & Hu, L. (2016). Flexible, solid-state, ion-conducting membrane with 3D garnet nanofiber networks for lithium batteries. *Proceedings of the National Academy of Sciences of the United States of America*, 113(26), 7094–7099; doi:10.1073/pnas.1600422113
- Ghani, N. A. A., Othaman, R., Ahmad, A., Anuar, F. H., & Hassan, N. H. (2019). Impact of purification on iota carrageenan as solid polymer electrolyte. *Arabian Journal of Chemistry*, 12(3), 370–376; doi:10.1016/j.arabj.2018.06.008
- Ghorpade, V. S., Yadav, A. V., Dias, R. J., Mali, K. K., Pargaonkar, S. S., Shinde, P. V., & Dhane, N. S. (2018). Citric acid crosslinked carboxymethylcellulose-poly(ethylene glycol) hydrogel films for delivery of poorly soluble drugs. *International Journal of Biological Macromolecules*, 118, 783–791; doi:10.1016/j.ijbiomac.2018.06.142
- Gupta, S., & Varshney, P. K. (2019). Effect of plasticizer on the conductivity of carboxymethyl cellulose-based solid polymer electrolyte. *Polymer Bulletin*, 76(12), 6169–6178; doi:10.1007/s00289-019-02714-1
- Jiang, J., Pan, H., Lin, W., Tu, W., & Zhang, H. (2019). UV-induced semi-interpenetrating polymer electrolyte membrane for elevated-temperature all-solid-state lithium-ion batteries. *Materials Chemistry and Physics*, 236, 121781; doi:10.1016/j.matchemphys.2019.121781
- Kanafi, N. M., Rahman, N. A., & Rosdi, N. H. (2019). Citric acid cross-linking of highly porous carboxymethyl cellulose/poly(ethylene oxide) composite hydrogel films for controlled release applications. *Materials Today: Proceedings*, 7, 721–731; doi:10.1016/j.matpr.2018.12.067
- Koops, C. G. (1951). On the dispersion of resistivity and dielectric constant of some semiconductors at audiofrequencies. *Physical Review*, 83(1), 121–124; doi:10.1103/PhysRev.83.121
- Kumar, M., & Srivastava, N. (2015). Conductivity and dielectric investigation of NH₄I-doped synthesized polymer electrolyte system. *Ionics*, 21(5), 1301–1310; doi:10.1007/s11581-014-1294-x
- Lehmann, M. L., Yang, G., Nanda, J., & Saito, T. (2020). Well-designed crosslinked polymer electrolyte enables high ionic conductivity and enhanced salt solvation. *Journal of The Electrochemical Society*, 167(7), 070539; doi:10.1149/1945-7111/ab7c6e
- Ma, X., Yu, J., He, K., & Wang, N. (2007). The effects of different plasticizers on the properties of thermoplastic starch as solid polymer electrolytes. *Macromolecular Materials and Engineering*, 292(4), 503–510; doi:10.1002/mame.200600445
- Mali, K. K., Dhawale, S. C., Dias, R. J., Dhane, N. S., & Ghorpade, V. S. (2018). Citric acid crosslinked carboxymethyl cellulose-based composite hydrogel films for drug delivery. *Indian Journal of Pharmaceutical Sciences*, 80(4), 657–667. doi:

- 10.4172/pharmaceutical-sciences.1000405
- Mazuki, N. F., Abdul Majeed, A. P. P., Nagao, Y., & Samsudin, A. S. (2020). Studies on ionic conduction properties of modification CMC-PVA based polymer blend electrolytes via impedance approach. *Polymer Testing*, 81, 106234; doi:10.1016/j.polymertesting.2019.106234
- Mazuki, N. F., Fuzlin, A. F., Saadiah, M. A., & Samsudin, A. S. (2019). An investigation on the abnormal trend of the conductivity properties of CMC/PVA-doped NH₄Cl-based solid biopolymer electrolyte system. *Ionics*, 25(6), 2657–2667; doi:10.1007/s11581-018-2734-9
- Meabe, L., Huynh, T. V., Mantione, D., Porcarelli, L., Li, C., O'Dell, L. A., Sardon, H., Armand, M., Forsyth, M., Mecerreyes, D. (2019). UV-cross-linked poly(ethylene oxide carbonate) as free standing solid polymer electrolyte for lithium batteries. *Electrochimica Acta*, 302, 414–421; doi:10.1016/j.electacta.2019.02.058
- Megha, R., Ravikiran, Y. T., Kotresh, S., Vijaya Kumari, S. C., Raj Prakash, H. G., & Thomas, S. (2018). Carboxymethyl cellulose: An efficient material in enhancing alternating current conductivity of HCl doped polyaniline. *Cellulose*, 25(2), 1147–1158; doi:10.1007/s10570-017-1610-5
- Mei, B. A., Munteshari, O., Lau, J., Dunn, B., & Pilon, L. (2018). Physical interpretations of nyquist plots for EDLC electrodes and devices. *Journal of Physical Chemistry C*, 122(1), 194–206; doi:10.1021/acs.jpcc.7b10582
- Nan, N. F. C., Zainuddin, N., & Ahmad, M. (2019). Preparation and swelling study of CMC hydrogel as potential superabsorbent. *Pertanika Journal of Science and Technology*, 27(1), 489–498.
- Ndruru, S. T. C. L., Wahyuningrum, D., Bundjali, B., & Made Arcana, I. (2019). Green synthesis of [EMIm]Ac ionic liquid for plasticizing mc-based biopolymer electrolyte membranes. *Bulletin of Chemical Reaction Engineering & Catalysis*, 14(2), 345–357; doi:10.9767/bcrec.14.2.3074.345-357
- Ng, B. C., Wong, H. Y., Chew, K. W., & Osman, Z. (2011). Development and characterization of Poly-ε-caprolactone-based polymer electrolyte for lithium rechargeable battery. *International Journal of Electrochemical Science*, 6(9), 4355–4364.
- Nyuk, C. M., & Mohd Isa, M. I. N. (2017). Solid biopolymer electrolytes based on carboxymethyl cellulose for use in coin cell proton batteries. *Journal of Sustainability Science and Management*, 2017(2), 42–48. <https://oarep.usim.edu.my/jspui/handle/123456789/13828>
- Perumal, P., Christopher Selvin, P., Selvasekarapandian, S., & Abhilash, K. P. (2019). Bio-host pectin complexed with dilithium borate based solid electrolytes for polymer batteries. *Materials Research Express*, 6(11), 115513; doi:10.1088/2053-1591/ab4724
- Putro, P. A., Sulaeman, A. S., & Erizal. (2019). Synthesis and characterization of swelling properties superabsorbent hydrogel carboxymethylcellulose-g-poly (acrylic acid)/natrium alginate cross-linked by gamma-ray irradiation technique. *Journal of Physics: Conference Series*, 1171, 012011; doi:10.1088/1742-6596/1171/1/012011
- Putro, P. A., Sulaeman, A. S., & Maddu, A. (2021). The role of C-dots/(MnO₂)_x (x = 0, 2, 4, mM) on enhancing the ion transport in poly (ethylene oxide) based solid polymer electrolytes: The Optical and electrical characteristics. *Journal of Physics: Conference Series*, 1805, 012020; doi:10.1088/1742-6596/1805/1/012020
- Putro, Permono Adi, Yudasari, N., Irdawati, Y., Sulaeman, A. S., & Maddu, A. (2021). Reducing the electrical conductivity of ZnO/Ag nanofiller for solid polymer electrolytes prepared by laser ablation in polylactic acid solution. *Jurnal Fisika Dan Aplikasinya*, 17(2), 41; doi:10.12962/j24604682.v17i2.8135
- Ravi, M., Song, S., Wang, J., Nadimicherla, R., & Zhang, Z. (2016). Preparation and characterization of biodegradable poly(ε-caprolactone)-based gel polymer electrolyte films. *Ionics*, 22(5), 661–670; doi:10.1007/s11581-015-1586-9
- Ren, W., Huang, Y., Xu, X., Liu, B., Li, S., Luo, C., Li, X., Wang, M., Cao, H. (2020). Gel polymer electrolyte with high performances based on polyacrylonitrile composite natural polymer of lignocellulose in lithium ion battery. *Journal of Materials Science*, 55(26), 12249–12263; doi:10.1007/s10853-020-04888-w
- Saadiah, M. A., & Samsudin, A. S. (2018). Electrical study on carboxymethyl cellulose-polyvinyl alcohol based bio-polymer blend electrolytes. *IOP Conference Series: Materials Science and Engineering*, 342(1), 012045; doi:10.1088/1757-899X/342/1/012045
- Salleh, N. S., Aziz, S. B., Aspanut, Z., & Kadir, M. F. Z. (2016). Electrical impedance and conduction mechanism analysis of biopolymer electrolytes based on methyl cellulose doped with ammonium iodide. *Ionics*, 22(11), 2157–2167; doi:10.1007/s11581-016-1731-0
- Samsudin, A. S., Aziz, M. I. A., & Isa, M. I. N. (2012). natural polymer electrolyte system based on sago: Structural and transport behavior characteristics. *International Journal of Polymer Analysis and Characterization*, 17(8), 600–607; doi:10.1080/1023666X.2013.723846
- Samsudin, A. S., Lai, H. M., & Isa, M. I. N. (2014). Biopolymer materials based carboxymethyl cellulose as a proton conducting biopolymer electrolyte for application in rechargeable proton battery. *Electrochimica Acta*, 129, 1–13; doi:10.1016/j.electacta.2014.02.074
- Samsudin, A. M., Wolf, S., Roschger, M., & Hacker, V. (2021). Poly(vinyl alcohol)-based anion exchange membranes for alkaline direct ethanol fuel cells. *International Journal of Renewable Energy Development*, 10(3), 435–443; doi:10.14710/ijred.2021.33168
- Scrosati, B., & Garche, J. (2010). Lithium batteries: Status, prospects and future. *Journal of Power Sources*, 195(9), 2419–2430; doi:10.1016/j.jpowsour.2009.11.048
- Shyly, P. M., Roy, S. D. D., Thiravetyan, P., Thanikaikarasan, S., Sebastian, P. J., Eapen, D., & Shajan, X. S. (2014). Investigations on the effect of chitin Nanofiber in PMMA Based solid polymer electrolyte systems. *Journal of New Materials for Electrochemical Systems*, 17(3), 147–152; doi:10.14447/jnmes.v17i3.405
- Sim, L. H., Gan, S. N., Chan, C. H., & Yahya, R. (2010). ATR-FTIR studies on ion interaction of lithium perchlorate in polyacrylate/poly(ethylene oxide) blends. *Spectrochimica Acta - Part A: Molecular and Biomolecular Spectroscopy*, 76(3–4), 287–292; doi:10.1016/j.saa.2009.09.031
- Stavriniidou, E., Sessolo, M., Winther-Jensen, B., Sanaur, S., & Malliaras, G. G. (2014). A physical interpretation of impedance at conducting polymer/electrolyte junctions. *AIP Advances*, 4(1); doi:10.1063/1.4863297
- Sulaeman, A. S., Maddu, A., Wahyudi, S. T., & Rifai, A. (2021). Salt concentration effect on electrical and dielectric properties of solid polymer electrolytes based carboxymethyl cellulose for lithium-ion batteries. *Biointerface Research in Applied Chemistry*, 12(5), 6114–6123; doi:10.33263/BRIAC125.61146123
- Sun, B., Mindemark, J., Edström, K., & Brandell, D. (2014). Polycarbonate-based solid polymer electrolytes for Li-ion batteries. *Solid State Ionics*, 262, 738–742; doi:10.1016/j.ssi.2013.08.014
- Sunandar, M., Yulianti, E., Deswita, D., & Sudaryanto, S. (2019). Study of solid polymer electrolyte based on biodegradable polymer polycaprolactone. *Malaysian Journal of Fundamental and Applied Sciences*, 15(3), 467–471; doi:10.11113/mjfas.v15n3.1185
- Tarascon, J. M., & Armand, M. (2001). Issues and challenges facing rechargeable lithium batteries. *Nature*, 414(6861), 359–367; doi:10.1038/35104644
- Tripathi, N., Shukla, A., Thakur, A. K., & Marx, D. T. (2020). Dielectric modulus and conductivity scaling approach to the analysis of ion transport in solid polymer electrolytes. *Polymer Engineering and Science*, 60(2), 297–305; doi:10.1002/pen.25283
- Verdier, N., Lepage, D., Zidani, R., Prébé, A., Aymé-Perrot, D., Pellerin, C., Dollé, M., & Rochefort, D. (2020). Cross-linked polyacrylonitrile-based elastomer used as gel polymer electrolyte in Li-ion battery. *ACS Applied Energy Materials*, 3(1), 1099–1110; doi:10.1021/acsae.9b02129
- Verma, M. L., & Sahu, H. D. (2017). Study on ionic conductivity

- and dielectric properties of PEO-based solid nanocomposite polymer electrolytes. *Ionics*, 23(9), 2339–2350; doi:[10.1007/s11581-017-2063-4](https://doi.org/10.1007/s11581-017-2063-4)
- Wang, X., Zeng, W., Hong, L., Xu, W., Yang, H., Wang, F., Duan, H., Tang, M., & Jiang, H. (2018). Stress-driven lithium dendrite growth mechanism and dendrite mitigation by electroplating on soft substrates. *Nature Energy*, 3(3), 227–235; doi:[10.1038/s41560-018-0104-5](https://doi.org/10.1038/s41560-018-0104-5)
- Wivanius, N., & Budianto, E. (2015). Sintesis dan karakterisasi hidrogel superabsorben kitosan Poli(N-Vinilkaprolaktam) (Pnvc) dengan metode full IPN (Interpenetrating Polymer Network). *Pharmaceutical Sciences and Research*, 2(3), 152–168; doi:[10.7454/psr.v2i3.3483](https://doi.org/10.7454/psr.v2i3.3483)
- Yap, Y. L., You, A. H., Teo, L. L., & Hanapei, H. (2013). Inorganic filler sizes effect on ionic conductivity in polyethylene oxide (PEO) composite polymer electrolyte. *International Journal of Electrochemical Science*, 8(2), 2154–2163.
- Yuan, X.-Z., Song, C., Wang, H., & Zhang, J. (2010). Electrochemical impedance spectroscopy in pem fuel cells fundamentals and applications. Springer-Verlag, London.



© 2022. The Author(s). This article is an open access article distributed under the terms and conditions of the Creative Commons Attribution-ShareAlike 4.0 (CC BY-SA) International License (<http://creativecommons.org/licenses/by-sa/4.0/>)